Advances in Materials Research, *Vol. 14, No. 4 (2025) 000-000*
https://doi.org/10.12989/amr.2025.14.4.000

Characterization of activated carbon produced by bio-waste material

Dipali L. Patil* and Namdeo A. Hedaoo[a]

Department of Civil Engineering, COEP Technological University, Pune-411005, Maharashtra, India

(*Received May 15, 2025, Revised July 31, 2025, Accepted August 30, 2025*)

Abstract. The rising demand for activated carbon (AC) in filtration, environmental protection, and energy storage necessitates cost-effective and sustainable production methods. Conventional AC production relies on non-renewable resources, leading to environmental concerns and high costs. This study addresses this gap by utilizing biowaste materials, specifically sawdust and walnut shells, for AC synthesis through chemical activation using phosphoric acid. The carbonization process was conducted at 300°C, 600°C, and 700°C, followed by detailed characterization using Scanning Electron Microscopy (SEM), Fourier Transform Infrared Spectroscopy (FTIR), Proximate Analysis, and CHNSO analysis. Adsorption capacity was assessed using iodine value measurements, which identified 600°C as the optimal temperature for activation. Carbon, hydrogen, Nitrogen, sulfur, and oxygen (CHNSO) analysis revealed that walnut shell-derived AC contained 36.5% more carbon than sawdust-derived AC, making it superior for energy storage applications. SEM analysis further confirmed a more heterogeneous structure with smaller pores in walnut shell AC, enhancing its adsorption efficiency. The study underscores the potential of biowaste-derived AC as a sustainable alternative, reducing reliance on conventional carbon sources and promoting circular economy principles. These findings contribute to waste valorization efforts, demonstrating an eco-friendly approach to producing high-performance AC while addressing environmental concerns associated with agricultural and industrial waste. Future research should focus on scaling production, optimizing activation processes, and exploring practical applications of biowaste-derived AC in industrial and environmental sectors to enhance its commercial viability.

Keywords: activated carbon; adsorption capacity; biowaste; chemical activation; sustainable production

1. Introduction

Activated carbon (AC) is a highly porous material characterized by exceptional physicochemical properties, with a surface area ranging between 600 and 2000 m^2/g (Yunus 2020). Owing to its superior adsorption capabilities, AC is extensively employed in applications such as water purification, air filtration, and energy storage (Ahmed 2022). Traditionally, AC has been manufactured from carbon-rich raw materials, including coal, wood, and coconut shells. However, the dependence on non-renewable resources has raised significant concerns regarding environmental

*Ph.D. Student, E-mail: dlp21.civil@coeptech.ac.in
[a]Associate Professor, E-mail: nah.civil@coeptech.ac.in

http://www.techno-press.org/?journal=amr&subpage=5 ISSN: 2234-0912 (Print), 2234-179X (Online)

degradation and resource depletion, thereby necessitating the exploration of sustainable alternatives.

In recent years, researchers have increasingly concentrated on the utilization of biowaste for the production of AC. Biowaste, which encompasses materials such as sawdust and walnut shells, represents an abundant and underutilized resource that offers a sustainable solution for waste management while serving as an eco-friendly precursor for AC synthesis (Wong 2018). The conversion of biomass into AC mitigates environmental pollution and enhances its commercial value by transforming waste into high-performance adsorbents. This sustainable approach is congruent with the principles of a circular economy, aiming to minimize waste and maximize resource utilization (Gorbounov *et al*. 2023).

The characteristics of AC, including pore size, surface area, and adsorption capacity, are significantly influenced by the choice of raw material and the activation process employed (Bedane *et al*. 2023). AC may be synthesized through either physical or chemical activation. Physical activation entails high-temperature pyrolysis followed by treatment with oxidizing gases, resulting in a durable form of AC characterized by moderate adsorption capacity (Yahya 2015). Conversely, chemical activation employs activating agents such as phosphoric acid (H_3PO_4), potassium hydroxide (KOH), or zinc chloride ($ZnCl_2$) to enhance the porosity and surface characteristics of AC at reduced temperatures (Kim, 2001). Although chemical activation yields higher carbon content and improved adsorption properties, it necessitates extensive washing to eliminate residual chemicals (Lozano-Castello 2001). In addition to its established roles in water purification, air filtration, and energy storage, activated carbon has garnered increasing attention for its application in carbon dioxide (CO_2) capture due to its high surface area, adjustable pore structure, and surface functional groups. Recent studies have demonstrated the feasibility of using biomass-derived activated carbon for efficient CO_2 adsorption in post-combustion and direct air capture processes, offering low-cost and sustainable alternatives to synthetic adsorbents (Zhao *et al*. 2024, Chen *et al*. 2024, Li *et al*. 2024, Wang *et al*. 2025, Liu *et al*. 2024). This adds another dimension to the relevance of biowaste-derived activated carbon in addressing environmental challenges such as greenhouse gas mitigation.

This study focuses on producing AC from sawdust and walnut shells utilizing phosphoric acid activation at 300°C, 600°C, and 700°C. This research aims to optimize the activation parameters and evaluate the physicochemical properties of the resultant AC. Characterization techniques such as Scanning Electron Microscopy (SEM), Fourier Transform Infrared Spectroscopy (FTIR), CHNSO analysis, and proximate analysis are employed to assess the surface morphology, elemental composition, and adsorption performance of the synthesized AC.

Significance of the Study

The significance of this study resides in its contribution to sustainable waste management and efficient resource utilization. This research establishes an eco-friendly alternative to conventional AC production by converting biowaste into high-performance AC, thereby reducing reliance on non-renewable materials. The optimized activation process enhances the adsorption efficiency of AC, rendering it suitable for environmental applications, including water treatment and air purification. Furthermore, the findings provide valuable insights into the influence of activation temperature on the properties of AC, thereby paving the way for future advancements in biowaste-derived adsorbents. This study supports the global transition toward sustainable material development, reinforcing the potential of biowaste as a viable resource for producing cost-effective and high-quality AC.

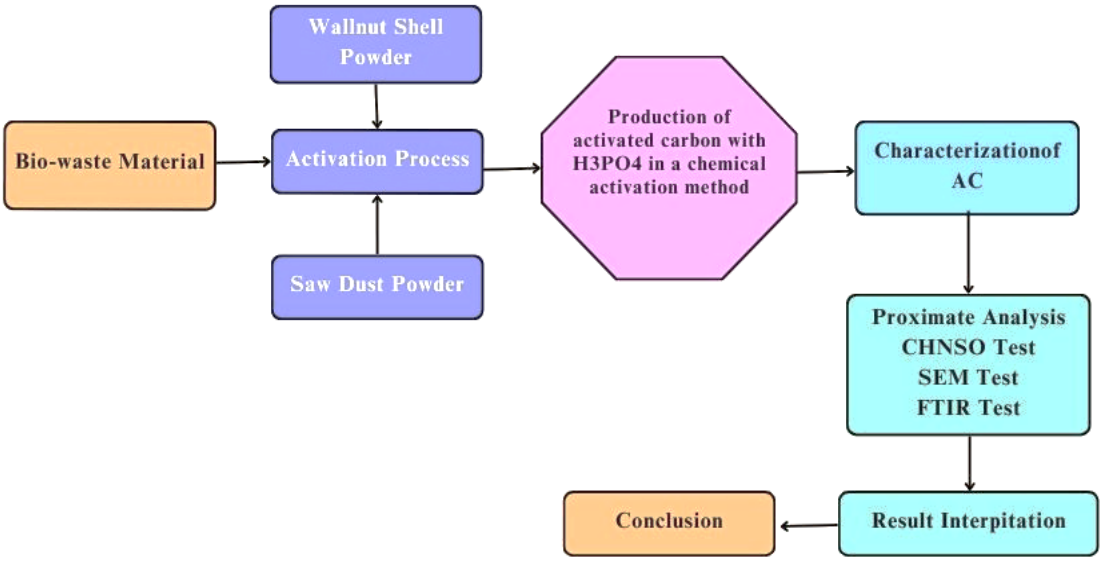

Fig. 1 Research methodology

2. Research methodology

As illustrated in Fig. 1, this study investigates the production of activated carbon (AC) from biowaste sawdust and walnut shells using phosphoric acid (H_3PO_4) as a chemical activating agent. The process involved carbonization at 300°C, 600°C, and 700°C for 1 hour in a muffle furnace, followed by chemical activation using a fixed 1 M H_3PO_4 solution for 24 hours. This acid concentration was kept constant to isolate the effect of temperature on AC properties. Post-activation, the samples were washed with distilled water to remove residual acid and then oven-dried at 155–160°C. Yield was recorded to evaluate thermal efficiency at each temperature. The AC was characterized using SEM for surface morphology and pore structure, FTIR for functional groups, CHNSO analysis for elemental composition, Proximate analysis for moisture, ash, volatile matter, and fixed carbon, and iodine number testing for adsorption capacity and microporosity. This method ensures a detailed evaluation of biowaste-derived AC and its suitability for environmental and energy storage applications. While H_3PO_4 dosage was fixed in this study, its variation is suggested for future optimization.

3. Production of activated carbon

3.1 Materials

AC is derived from the remnants of sawdust and walnut shells. These materials were acquired from a furniture-making establishment in Pune, India, and the dried fruit sector. These leftovers are selected based on their unique attributes, which include a substantial amount of carbon, wide availability, and cost-effectiveness. Shells from nuts, such as almonds and walnuts, are discarded byproducts from various sectors and can be collected collectively for repurposing. Conversely,

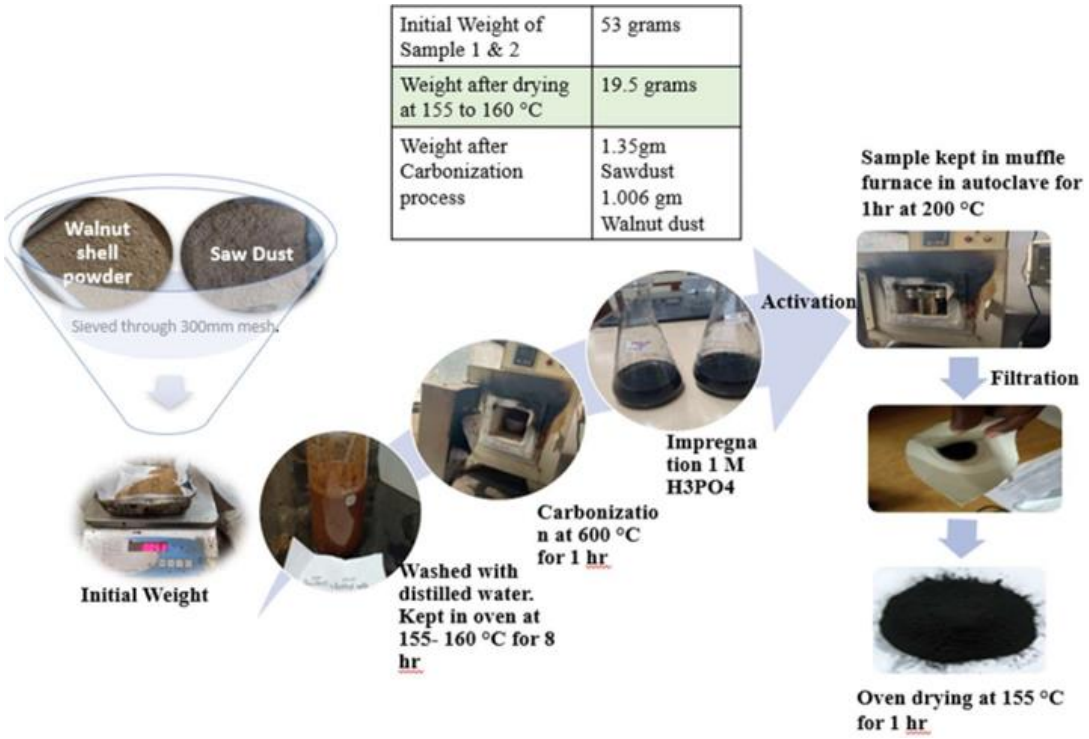

Fig. 2 Process of making activated carbon

sawdust is a plentiful and economical material made of lignocellulose. Additionally, it is a residue from timber processing activities such as shaping and smoothing.

3.2 Procedure of making activated carbon from sawdust and walnut shell

As shown in Fig. 2, the raw materials selected, namely sawdust and walnut shells, are chosen due to their elevated carbon content. In the initial stage, the materials were washed using distilled water to eradicate impurities. After removing moisture content, the specimens were desiccated in an oven set at a temperature range of 155-160°C for 5 hours. Following this step, the materials underwent carbonization at varying temperatures - 300°C, 600°C, and 700°C - for 1 hour each, under an inert atmosphere within a muffle furnace to achieve the desired content. Post carbonization, all samples were subjected to chemical activation using 1 mol of phosphoric acid (H3PO4) for 24 hours. After the chemical activation process, the activated samples were filtered through filter paper and rinsed with distilled water to eliminate residual acid that could trigger undesired degradation reactions. Finally, the activated samples were again dried in an oven at 155°C, producing the final product – AC (Temitayo 2021).

4. Characterization of activated carbon

Kenaf fibers were ground and sieved using mesh size 40 (400µm). The fibers were added to nylon pellet at weight ratios based on the predetermined study groups which were (0.1%, 0.3%,

0.5%, and 1% of kenaf fibers concentrations). The mix was processed and extruded thermally at 250℃ using thermal extruding machine. The study specimens were printed by Creality Ender 3 Neo FDM 3D printer, China, using the extruded filaments for the experimental groups, and the as-received nylon filament for printing the control group. The specimens were designed by DesignSpark Mechanical 6.0.3 software. Rectangular shape with dimensions of 100mm length, 10mm width, and 2mm thickness, was designed for the flexural strength test following ASTM D790 while the dimensions were adapted within a permissible range. A cylinder shape with dimensions of 30mm height and 10mm in diameter was designed for the compressive strength test following the general procedure of ASTM D695. The height-to-diameter ratio (3:1) was selected based on material stiffness and testing constraints, and no buckling was observed during testing. The Standard Tessellation Language (STL) file was sliced by PrusaSlicer 2.6.1 software before being transferred to the printer. The printing specifications are illustrated in Table 1. The total sample size was determined by G*power software (version 3.1.9.4). A power analysis for One Way ANOVA test indicated that the minimum sample size to yield a statistical power of at least 0.8 with an alpha of 0.05 and a medium effect size (d=0.5) is 55. Fig. 1 shows the study groups.

4.1 CHNSO analysis

By analyzing its carbon, hydrogen, nitrogen, and sulfur content, examining AC through CHNSO testing is essential for determining its composition and properties. Recent research by the authors (De Souza *et al.* 2021) indicates that thermocouple sensors' cardboard tubes can be transformed into AC with a carbon content measuring 39.29%. Studies conducted by the authors (Li 2019) revealed that sulfur-impregnated AC effectively controls off-gas mercury emissions, achieving remarkable mercury removal rates of up to 99.999%. Moreover, using an activated carbon-based system for drug disposal has proven successful in deactivating medications, demonstrating the material's impressive adsorption capabilities, as highlighted in research studies (Soelberg 2007). These discoveries underscore the various applications and significance of CHNSO testing in evaluating the efficacy and quality of AC materials for diverse environmental and industrial uses.

4.2 SEM Analysis

SEM analysis of AC provides crucial insights into its surface morphology and structure. Researchers demonstrated that AC from waste tires exhibited a highly porous nature with a large surface area suitable for adsorption applications (Muttil *et al*. 2023). Energy-dispersive X-ray spectroscopy (EDS) was used to determine the composition of the element (Vernon, 2000). Similarly, studies by the authors highlighted the irregular and porous surface structure of AC produced from cardboard tubes, showing a high BET surface area of 468.9 m2 g−1 (Kunusa *et al*. 2021). Furthermore, research by researchers indicated that SEM analysis of activated charcoal from palm oil waste revealed varying pore sizes depending on the activation temperature, with the largest pores observed at 850°C (De Souza *et al.* 2021). These findings collectively emphasize the importance of SEM analysis in characterizing AC's surface morphology and porosity derived from different precursor materials for diverse applications.

4.3 Iodine number measurement

The iodine number measurement of AC is a crucial parameter that reflects its adsorption capacity (Temitayo 2021). Various studies have highlighted the significance of iodine number determination

in assessing the quality and effectiveness of activated carbon. For instance, researchers emphasize the importance of iodine value falling within the 1000-1400 mg/g range for AC used in gas mercury measurement (Huang and Yudong 2019). Additionally, studies discuss the impact of different preparation conditions, such as carbonization temperature, time, and impregnation ratio, on the iodine number of activated carbon, with optimal values identified for maximum adsorption capacity (Shrestha 2018, Kaya *et al*. 2018). The iodine number was determined by using Eq. (1)

$$Iodine\ value = \frac{M(V_B - V_A)}{2W} \quad (1)$$

where,

M = Thiosulphate Molarity.

VB= Thiosulphate volume at blank titration

VA= Thiosulphate volume for Activated Carbon

W = Weight of Activated Carbon

4.4 Moisture content

Determining the moisture content of AC produced from biowaste is a crucial parameter in assessing its quality. Various studies have investigated the production of AC from different biowastes like areca nut waste (Batu *et al*. 2022), mixed sugarcane bagasse and Rambutan twigs (Ariany 2018), sago residues (Kunusa *et al*. 2021), urban organic waste (Haji 2013), and organic waste with high water content (Min and Li 2022). The moisture content of AC plays a significant role in its adsorption capacity and overall effectiveness. Research findings indicate that moisture content values ranged from 1.11% to 7.17% in different biowaste-derived activated carbons, highlighting this parameter's importance in determining the final product's quality and performance. Proper control and measurement of moisture content are essential in optimizing the production process and ensuring the desired characteristics of the activated carbon. Both AC samples, weighing 10g each, were placed in the crucible and weighed. Subsequently, they were heated for three hours in an oven at 105–110°C. The samples were then cooled in a desiccator, and the weight of the dried samples with the crucible was recorded. Eq. (2) was used to calculate the moisture content (Temitayo 2021).

$$Moisture\ Content(\%) = \frac{A - B}{\mathrm{Ws}} \quad (2)$$

where,

A = weight of empty crucible + original sample weight

B = weight of empty crucible + dried sample weight

W_S = weight of the original sample

4.5 Ash content

Numerous research studies have underscored the importance of ash content in assessing the efficacy of activated carbon. In some previous studies (Ariany 2018), the significance of ash content and pH in producing premium AC was highlighted. Each of the two AC samples, weighing 5g, was placed in a crucible and weighed. Subsequently, the samples underwent a three-hour heating process at 900°C in a muffle furnace. After cooling in a desiccator, the samples were re-weighed to determine the ash content using equation 3 outlined by the study (Temitayo 2021).

$$Ash\ Content(\%) = \frac{C - D}{\mathrm{Ws}} \quad (3)$$

where,
C = weight of empty crucible + original sample weight
D = weight of empty crucible + dried sample weight
WS = weight of an original sample

4.6 Volatile content

Two samples containing 1g each were weighed using a crucible with a lid. Then, they were heated for 8 minutes at 900°C in a muffle furnace. After cooling, the samples were weighed again, and the volatile content was determined using equation 4 (Temitayo 2021).

$$Volatile\ Content(\%) = \frac{(100(A-B) - Mc(A-G)}{(A-G)(100-Mc)} * 100 \quad (4)$$

where,
A = Weight of empty crucible + original sample weight
B = Weight of empty crucible + dried sample weight
G = Empty crucible mass
Mc = Moisture content of the sample (%)

4.6 Bulk density

The methodology for determining bulk density was conducted by the guidelines provided by Sugumaran (2012), albeit with slight modifications. A glass vessel with a volume of 20 mL was employed to contain a specified amount of 42-mesh powdered carbon specimens sourced from SDAC, WNAC, and UC, subsequently subjected to drying in an oven at a temperature of 108°C for one night. After this, the cylinder was gently tapped to consolidate the carbon material for 2-3 minutes. The bulk density was computed using the prescribed formula in equation 5 and denoted in grams per millimetre.

$$Bulk\ Density = \frac{Mass\ of\ Sample\ (dry)}{Volume\ of\ Measuring\ Cylinder} * 100 \quad (5)$$

4.7 FTIR analysis

Spectrum One FTIR equipment and spectrum analysis software subjected the samples to FTIR analysis. 0.6g of AC and an equal volume of potassium bromide (KBr) were combined to prepare the sample. After this combination was ground into a uniform powder in a mortar, it was formed into very thin plates. These plates were placed into the spectrophotometer for examination with a wavenumber ranging from 4100 to 360 cm^{-1} (Patil and Hedaoo 2023, 2024, 2025).

5. Results and analysis

5.1 Proximate analysis

Fig. 3 shows the graph of carbonization temperature and iodine value, indicating that the iodine value increases with a rise in carbonization temperature up to 600°C. By reaching a temperature of

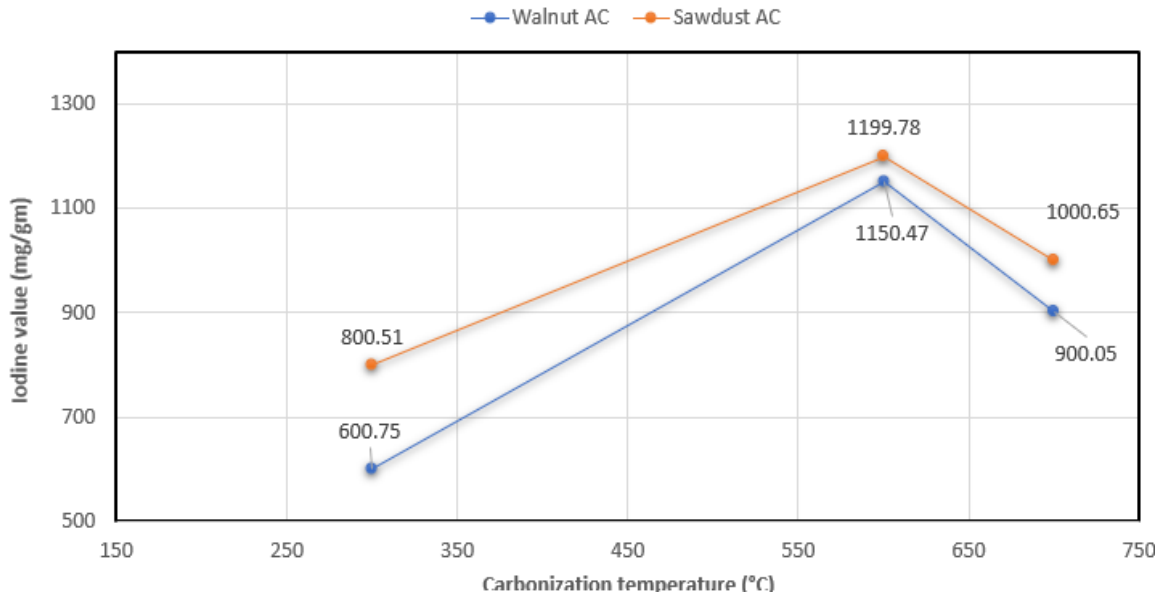

Fig. 3 The impact of activation temperature on iodine number

Table 1 Summary of activated carbon characteristics at different carbonization temperatures

Temperature (°C)	Biomass Type	Yield (%)	Moisture Content (%)	Ash Content (%)	Volatile Matter (%)	Iodine Value (mg/g)
300	Sawdust	42	7.2	5.5	12.3	110.40
300	Walnut Shell	38	6.9	4.8	13.5	102.60
600	Sawdust	33	6.8	4.0	7.89	150.47
600	Walnut Shell	30	5.8	3.0	10.82	1200.00
700	Sawdust	28	6.5	4.5	6.4	100.25
700	Walnut Shell	24	5.4	3.3	8.7	980.12

700°C, the iodine value decreases. This shows that the optimum temperature for carbonization is 600 °C.

The findings of the proximate analysis are presented in Table 1. The ACSNI 06-3730-1995 standard shows that the maximum ash content is 10%, the maximum moisture content is 15%, and the minimum iodine absorption is 750 mg/g. The moisture content was 5.8% in walnut AC and 6.8% in sawdust AC. The calculated ash content was 3% in walnut AC and 4% in acceptable sawdust AC. The volatile content in walnut AC is 10.8%, and sawdust AC contains 7.89% of volatile matter. All the parameters are in the acceptable range.

5.2 Iodine absorption analysis

The iodine number is a basic measurement to approximate the AC surface area at room temperature. It plays a crucial role in determining the permeability and adsorptive capacity of the material. The higher iodine values found in some carbon samples are mainly explained by a large

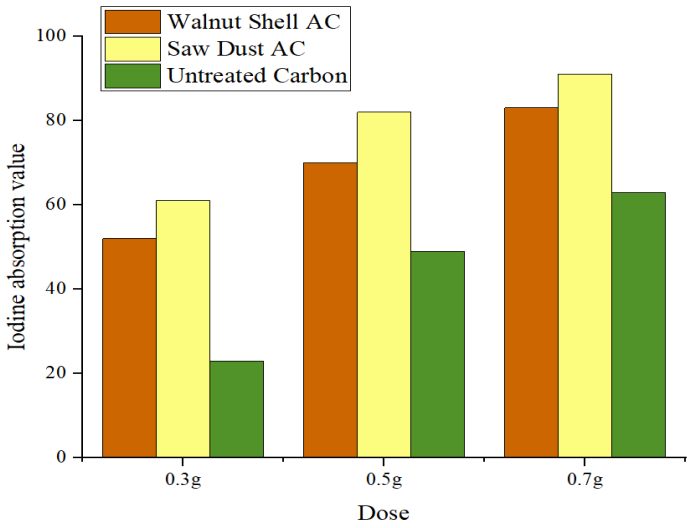

Fig. 4 Dose-wise Iodine absorption value

microporous structure and the possibility of a huge surface area due to aperture structure expansion (Ekpete 2011). The findings of iodine removal from different carbon samples dosed at 0.3g, 0.5g, and 0.7g are shown in Figure 4. iodine number determination, aliquots of carbon samples weighing 0.3g, 0.5g, and 0.7g were placed into 250 cm^3 conical flasks and treated with 10 cm^3 of 5% hydrochloric acid (HCl), followed by agitation. Subsequently, 100 mL of a stock iodine solution, prepared by dissolving 2.4 g of iodine and 4.0 g of potassium iodide (KI) in 1 liter of deionized water (DI) and previously standardized against a 0.1 M solution of sodium thiosulfate, was added to each flask. The resulting mixture was agitated for 20 minutes before filtration through filter paper. A 30 mL aliquot of the filtrate was then titrated with 0.1 M sodium thiosulfate solution, with starch serving as the indicator. The percent iodine adsorbed by each carbon was calculated using Equation 6 (Ekpete 2017).

$$\frac{[mL\ of\ Na_2S_2O_3\ in\ blank - \ mL\ of\ Na_2S_2O_3\ in\ sample]}{mL\ of\ Na_2S_2O_3\ in\ blank} * 100 \quad (6)$$

The findings clearly show that the iodine value of all samples rose as sample concentration increased. Of the concentrations used, SDAC had the greatest iodine value. The significant difference between UC and SDAC/WNAC is ascribed to a sizable microporous structure, most likely made possible by chemisorption processes during carbonization and activation. The activating agents' different reactivity rates cause the difference between SDAC and WNAC.

5.3 SEM Analysis

The surface morphologies of the produced AC were analyzed using SEM. Fig. 6(a)-(c) demonstrates SEM images of sawdust AC at 10000x, 5000x, and 1000x magnifications, respectively. Fig. 8(a)-(c) shows SEM images of walnut shell AC at 100x, 10kx, and 3kx magnifications, respectively. It can be seen that there are fine pores visible within the microstructure of AC. Walnut shell AC contains more pores than sawdust AC. There are several cavities on the external of the AC. The particles appeared to be randomly oriented and dispersed throughout the samples. The

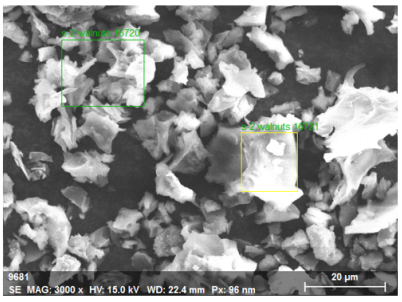

a)

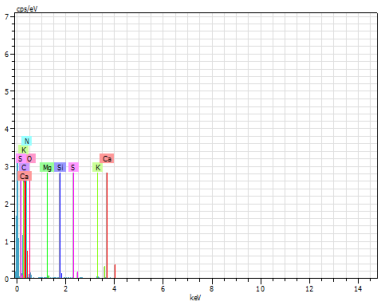

b)

Element	Atomic no.	Wt%
C	6	81.87
O	8	15.55
K	19	1.30
Ca	20	0.96
Mg	12	0.24
Si	14	0.08
N	7	0.00
S	16	0.00

c)

Fig. 5 EDS Spectrum of Walnut Shell AC: a) SEM Image b) EDS Spectrum c) Elemental Composition

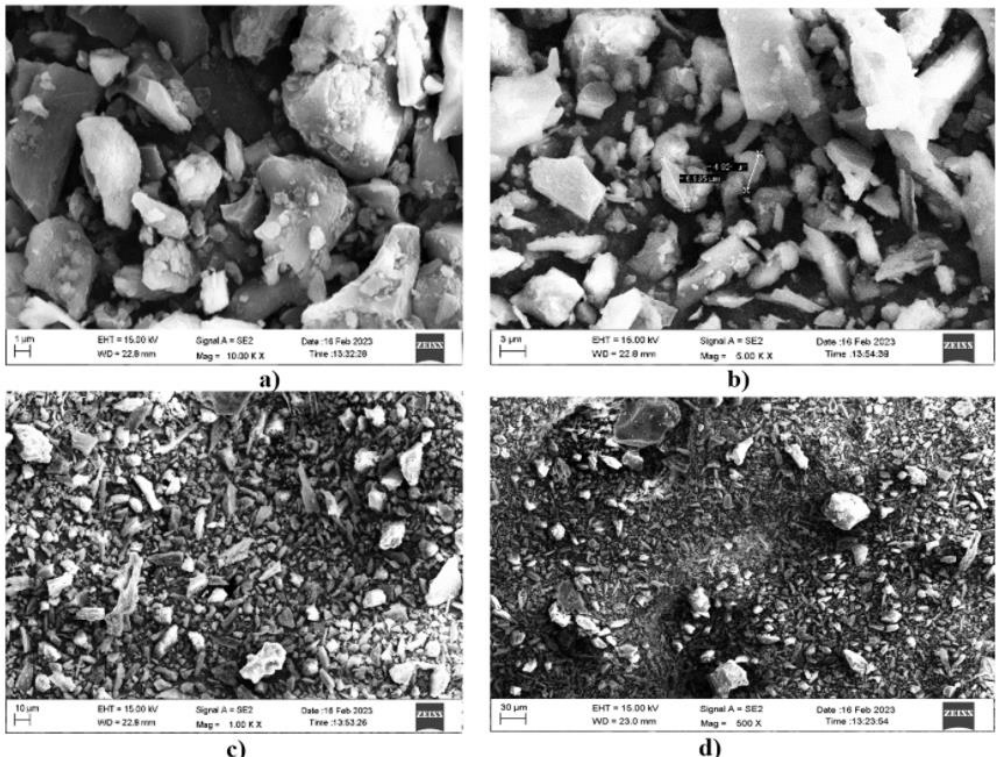

a) b) c) d)

Fig. 6 SEM image of Sawdust-AC a) $1\mu m(10KX)$ b) 3 $\mu m(5KX)$c) 10 μm(1KX), d) 30 μm(500X)

particle size of walnut AC was in the range of 5.17-20.62 µm, And that of sawdust AC was in the range of 2.5-11.48 µm.

5.4 Energy-dispersive spectroscopy (EDS)

EDS spectra were carried out to analyse the changes in the elemental composition of activated carbon. In Figures 5 and 7, the first image is SEM, the second is the EDS spectrum, and the third shows the walnut shell AC's and sawdust AC's elemental composition, respectively. The percentage of carbon in this composition is high, followed by oxygen.

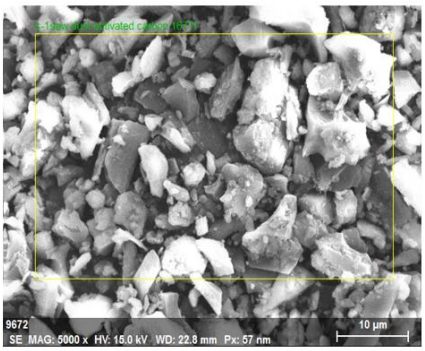

a)

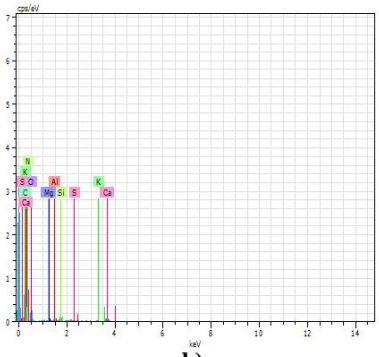

b)

Element	Atomic no.	Wt%
C	6	62.31
O	8	30.83
Ca	20	3.84
Si	14	1.53
Al	13	0.63
K	19	0.54
Mg	12	0.31
S	16	7

c)

Fig. 7 EDS Spectrum of Sawdust AC: a) SEM Image b) EDS Spectrum c) Elemental Composition

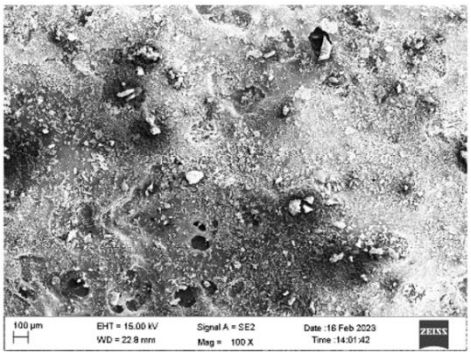

a)

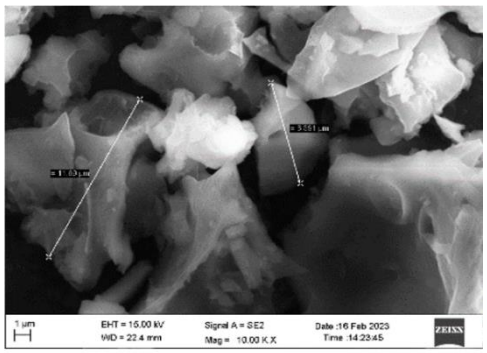

b)

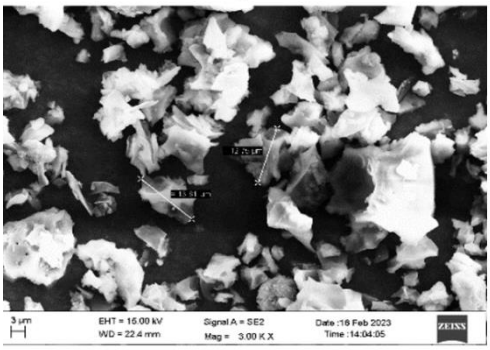

c)

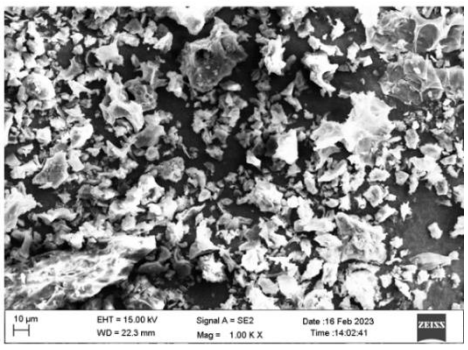

d)

Fig. 8 SEM image of Walnut shell-AC a) 100 μm(100X) b) 1 $\mu m(10KX)$ c) 3 μm $(3KX)$, d) 10 μm (1 KX)

5.5 CHSNO

The initial carbon content of sawdust and walnut shells was evaluated. Table No. 2 shows that walnut shells have a higher carbon content than sawdust.

Table 3 shows the CHNSO values of sawdust and walnut shell AC. The developed molecular

Table 2 Carbon content in raw materials

Specimen	Carbon %
Walnut shell	41.65
Sawdust	37.7

Table 3 CHNSO result

Specimen	Carbon %	Hydrogen %	Nitrogen %	Sulphur %	Oxygen %
Walnut shell AC	66.21	1.03	0.19	0.39	22.68
Sawdust AC	49.07	2.99	0.29	0.21	10.35

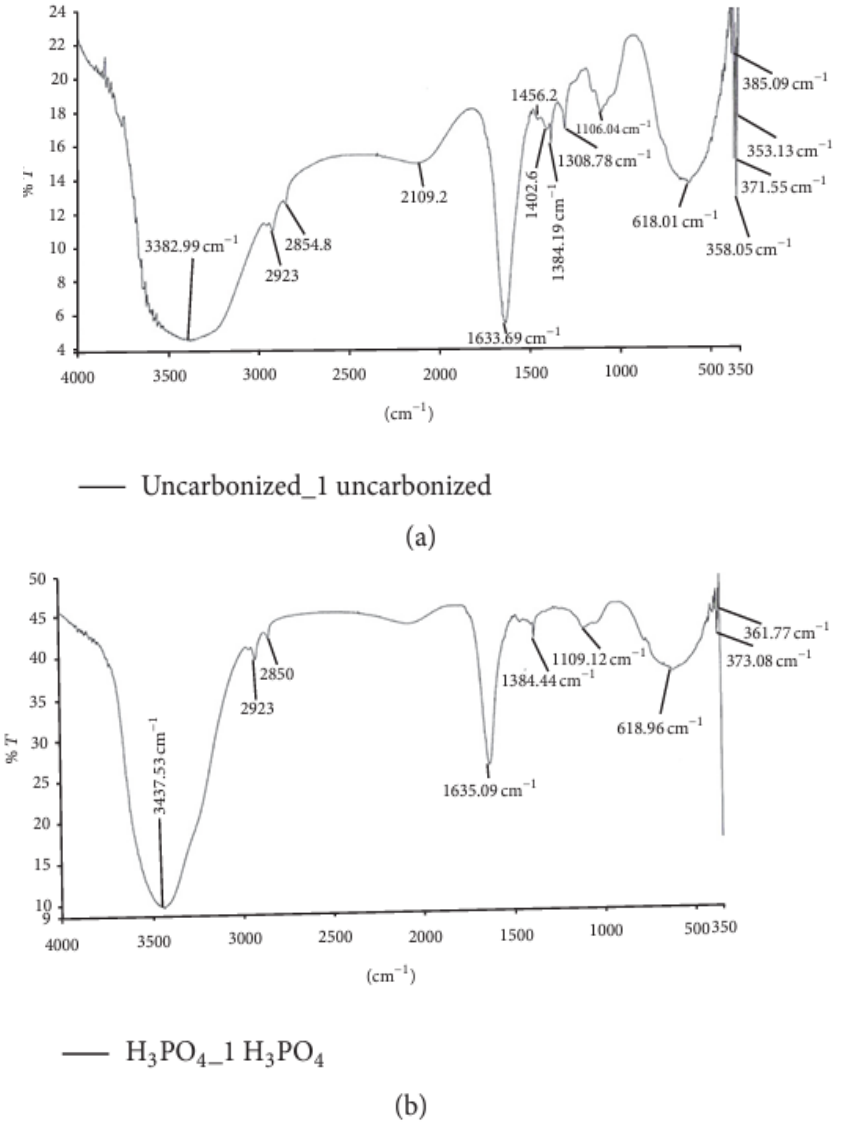

Fig. 9 (a) Spectra Analysis of UC (b) Spectra Analysis of SDAC and WNAC

formula (not a chemical formula) of the sawdust-AC $C_{625}H_{454}N_{11}SO_{99}$ and that of walnut shell-AC $C_{405}H_{75}NS_2O$ The number below represents the atom present in the element. The carbon content of walnut shell AC is higher than sawdust AC.

5.6 FTIR analysis

As seen in Figs. 9(a) and (b), the samples' Fourier transform infrared analysis reveals similar peaks and values, suggesting a single source origin. A few of the most notable peaks are explained here. Fig. 10(a) (UC) displayed a broad band extending from 3500 to 3000 cm^{-1}, whereas Fig. 10(b) SDAC and WNAC showed strong broadband signals at 3438 and 3437 cm^{-1}, respectively. Whereas the wideband signal in UC most likely came from hydroxyl groups, the signals in SDAC and WNAC correlated with alcohols' -OH group vibrations. C-H stretching vibrations were correlated with common peak positions of 2921 cm^{-1}, 2852 cm^{-1}, and 1382 cm^{-1} found in all samples. In SDAC and WNAC, bands in the 1633–1644% cm^{-1} range were noticeable, they were particularly strong in UC. The former was linked to C=C alkene stretching, while the latter was probably caused by C=O stretching vibrations, which might have come from amides. (Patil and Hedaoo 2023)

Two bands in the 1100 to 1110 cm^{-1} range were found in SDAC, WNAC, and UC, while one unique band at 1035 cm^{-1} was found only in SDAC. The lack of bands at 1465 cm^{-1} and 1401 cm^{-1} in WNAC and SDAC, which were present in UC, implies that a chemical change happened during activation. Moreover, the band shifts and presence or absence changes in SDAC and WNAC show different responses to the corresponding activating agents.

5.7 Yield of activated carbon

The yield of activated carbon at different carbonization temperatures was determined based on the weight difference between the dried raw material and the final activated carbon product. The observed yields were as at 300°C: 38–42%, 600°C: 30–35% ,700°C: 24–28%. A general trend of decreasing yield with increasing temperature was observed, which is attributed to enhanced decomposition and volatilization of non-carbonaceous content at higher temperatures.

6. Conclusions

This study presents a sustainable approach to producing high-quality activated carbon from biowaste materials, specifically sawdust and walnut shells, using chemical activation with phosphoric acid (H_3PO_4). Walnut shell-derived AC exhibited 36.5% higher carbon content than sawdust-based AC, indicating superior performance for adsorption and energy storage applications. The study confirms that 600°C is the optimal activation temperature, yielding the highest iodine value and improved porosity. Activation at 700°C resulted in reduced adsorption efficiency due to possible structural degradation of the material. The AC samples were thoroughly characterized using SEM, FTIR, CHNSO, and proximate analysis. The walnut shell AC exhibited smaller pore sizes and a more heterogeneous structure, thereby enhancing its adsorptive behavior. These findings demonstrate the viability of converting agricultural waste into functional, eco-friendly adsorbents, supporting the circular economy by transforming waste into valuable products.

While the study highlights promising results, limitations include the absence of advanced characterization techniques, such as BET surface area analysis and X-ray diffraction (XRD), due to

equipment constraints. Future work should integrate these methods to gain a deeper understanding of surface area, crystallinity, and pore structure. Overall, this research validates the potential of biowaste-based AC for scalable applications in filtration, CO_2 capture, and energy storage sectors.

7. Future recommendations

Future research should prioritize the scaling up of activated carbon production to assess its industrial feasibility and economic viability. Investigating alternative chemical activators such as potassium hydroxide (KOH) and zinc chloride ($ZnCl_2$) could further enhance the porosity and adsorption capacity of biowaste-derived AC. Additionally, studies should investigate the impact of varying phosphoric acid (H_3PO_4) concentrations on pore structure development and overall carbon yield. To gain deeper insights into the material's structural properties, the application of advanced characterization techniques such as BET surface area analysis, X-ray diffraction (XRD), and nitrogen adsorption-desorption at 77 K is strongly recommended.

Lastly, real-world performance evaluation of the produced AC in applications such as wastewater treatment, air purification, and energy storage would help validate its practical utility and support its commercial deployment.

Acknowledgments

The research described in this paper was technically supported by the SPPU University, Pune, and the COEP Technological University, Pune by providing chemical laboratory.

References

Ahmed, A.S., Alsultan, M., Hameed, R.T., Assim, Y.F. and Swiegers, G.F. (2022), "High surface area activated charcoal for water purification", *J. Compos. Sci.*, **6**(10), 311. https://doi.org/10.3390/jcs6100311.

Ariany, Z.., Ghina, F., Hanum., A. and Sri, R. (2018), "The potential of AC derived from bio-char waste of bio-oil pyrolysis as an adsorbent", *Proceedings of the The 2nd International Conference on Engineering and Technology for Sustainable Development (ICET4SD 2017)*, 01029. https://doi.org/10.1051/MATECCONF/201815401029

Asadi-Sangachini, Z., Galangash, M.M., Younesi, H. and Nowrouzi, M. (2019), "The feasibility of cost-effective manufacturing activated carbon derived from walnut shells for large-scale CO2 capture", *Environ. Sci. Pollut. Res.*, **26**(26), 26542-26552. https://doi.org/10.1007/s11356-019-05842-3.

Batu, M.S., Naes, E. and Kolo, M.M. (2022), "Pembuatan karbon aktif dari limbah sabut pinang asal pulau timor sebagai biosorben logam ca dan mg dalam air tanah", *Jurnal Integrasi Proses*, **11**(1), 21-25. https://doi.org/10.36055/jip.v11i1.13181

Bedane, A., Guo, T., Shirani, B. and Xiao, H. (2023), "Textural characteristics of activated carbons prepared from agricultural residues-review", *Canadian J. Chem. Eng.*, **101**(12), 6718-6739. https://doi.org/10.1002/cjce.24960

Bouchelta, C., Medjram, M., Bertrand, O. and Bellat, J. (2008), "Preparation and characterization of AC from date stones by physical activation with steam", *J. Anal. Appl. Pyrolysis*, **82**(1), 70-77. https://doi.org/10.1016/J.JAAP.2007.12.009.

Coker, E.N., Lujan-Flores, X., Donaldson, B., Yilmaz, N. and Atmanli, A. (2023), "An assessment of the conversion of biomass and industrial waste products to activated carbon", *Energies*, **16**(4), 1606.

https://doi.org/10.3390/en1604160645

De Souza, C.C., Ciriano, M.R., da Silva, E.F., de Oliveira, M.A., da Silva Bezerra, A.C., Dumont, M.R., da Silva, A.C. and Machado, A.R.T. (2021), "Activated carbon obtained from cardboard tube waste of immersion thermocouple and adsorption of methylene blue", *Biomass Convers*. *Biorefinery*, **13**(4), 3297-3308. https://doi.org/10.1007/S13399-021-01428-7

Derya, Ö., Saban, B. and Mehmet, E.E. (2023), "Production of AC from the waste paper by chemical activation method", *Int*. *Adv*. *Res*. *Eng*. *J*., **7**(1), 52-61. https://doi.org/10.35860/iarej.1222591

Ekpete, O.A. and Horsfall Jr., M. (2011), "Preparation and characterization of AC derived from fluted pumpkin stem waste (Telfairia occidentalis hook f)", *Res*. *J*. *Chem*. *Sci*., **1**(3), 10-17.

Ekpete, O.A., Marcus, A.C. and Osi, V. (2017), "Preparation and characterization of activated carbon obtained from plantain (Musa paradisiaca) fruit stem", *J*. *Chem*., **2017**(1), 8635615. https://doi.org/10.1155/2017/8635615

Gorbounov, M., Petrovic, B., Ozmen, S., Clough, P. and Soltani, S.M. (2023), "Activated carbon derived from Biomass combustion bottom ash as solid sorbent for CO2 adsorption", *Chem*. *Eng*. *Res*. *Des*., **194**, 325-343. https://doi.org/10.1016/j.cherd.2023.04.057

Granbohm, H., Larismaa, J., Ali, S., Johansson, L.S. and Hannula, S.P. (2018), "Control of the size of silver nanoparticles and release of silver in heat treated SiO2-Ag composite powders", *Materials*, **11**(1), 80. https://doi.org/10.3390/ma11010080

Haji, A.G., Pari, G., Nazar, M. and Habibati, H. (2013), "Characterization of activated carbon produced from urban organic waste", *Int*. *J*. *Sci*. *Eng*., **5**(2), 89-94. https://doi.org/10.12777/IJSE.5.2.89-94

Heidari, N.Z., Dehghani, M., Heidari, M., Javedan, G., Ali, I. and Sillanpää, M. (2020), "Methods for preparation and activation of activated carbon: A review", *Environ*. *Chem*. *Lett*., **18**, 393-415. https://doi.org/10.1007/s10311-019-00955-0.

Kaya, M., Şahin, Ö. and Saka, C. (2018), "Preparation and TG/DTG, FT-IR, SEM, BET surface area, iodine number and methylene blue number analysis of activated carbon from pistachio shells by chemical activation". *Int*. *J*. *Chem*. *React*. *Eng*., **16**(2), 20170060. https://doi.org/10.1515/IJCRE-2017-0060

Khalil, H.P.S., Jawaid, M., Firoozian, P., Rashid, U., Islam, A. and Akil, H. M. (2013), "AC from various agricultural wastes by chemical activation with KOH: preparation and characterization", *J*. *Biobased Mater*. *Bioenergy*, **7**(6), 708-714. https://doi.org/10.1166/jbmb.2013.1379

Kim, J., Sohn, M., Kim, D., Sohn, S. and Kwon, Y. (2001), "Production of granular AC from waste walnut shell and itsadsorption characteristics for Cu(2+) ion", *J*. *Hazard*. *Mater*., **85**(3), 301-315. https://doi.org/10.1016/S0304-3894(01)00239-4.

Kunusa, W.R., Iyabu, H. and Abdullah, R. (2021), "FTIR, SEM and XRD analysis of activated carbon from sago wastes using acid modification", *J*. *Phys*. *Conference Series*, **1968**(1), 012014. https://doi.org/10.1088/1742-6596/1968/1/012014

Li, R, Zhu, G., Tong, Y., Gao, S., Liu, T. (2019), "Effects of the carbonization temperature and intermediate cooling mode on the properties of coal-based activated carbon", *Energy*, **273**, 127177. https://doi.org/10.1016/j.energy.2023.127177

Lozano-Castelló, D., Lillo-Ródenas, M., Cazorla-Amorós, D. and Linares-Solano, Á. (2001), "Preparation of activated carbons from Spanish anthracite. II. Activation by NaOH", *Carbon*, **39**, 751-759. https://doi.org/10.1016/S0008- 6223(00)00185-8.

Mahind, S.D. and Patil, D. (2022), "COVID-19—assessment of economic and schedule delay impact in Indian construction industry using regression method", *Proceedings of the Recent Trends in Construction Technology and Management: Select Proceedings of ACTM 2021*, 283-297, Singapore: Springer Nature Singapore. https://doi.org/10.1007/978-981- 19-2145-2_23

Muttil, N., Jagadeesan, S., Chanda, A., Duke, M. and Kumar Singh, S. (2024), "Characterisation of activated carbon derived from carbon black produced by the pyrolysis of waste tyres", *Adv*. *Mater*. *Proc*. *Technol*., **10**(4), 2957-2967. https://doi.org/10.1080/2374068x.2023.2192327

Oladimeji, T., Odunoye, B., Elehinafe, F., Obanla, O. and Odunlami, O. (2021), "Production of AC from sawdust and its efficiency in sewage water treatment", *Heliyon*, 7. https://doi.org/10.1016/j.heliyon.2021.e05960.

Patil, D. and Hedaoo, N. (2023), "Application of waste biaxially oriented polypropylene sandwiched graphene to enhance properties of asphalt mixes via a wet process", *Mater. Today Proc.*, In Press. https://doi.org/10.1016/j.matpr.2023.05.037

Patil, D. and Hedaoo, N. (2024), "Assessing the rheological behavior of bio-asphalt binder with integrating biowaste-derived activated carbon", *Civil Environ. Eng.*, **20**(2), 905-919. https://doi.org/10.2478/cee-2024-0066

Patil, D. and Hedaoo, N. (2025), "Effect of waste plastic and fiber modification on asphalt mixture properties", *J. Mater. Eng. Struct. JMES*, **12**(2), 127-137.

Patil, D. and Hedaoo, N. (2025), "Enhancing asphalt mixture properties through waste plastic and steel fiber additives: A comprehensive study", *J. Mater. Eng. Struct. JMES*, **12**(1), 5-19.

Patil, D., Shinde, S. and Hedaoo, N. (2025), "predicting creep and recovery responses of asphalt binders using machine learning models", *Airfield Highway Pavements*, 106-119. https://doi.org/10.1061/9780784486238.010

Sahira, J., Mandira, A., Prasad, B.P. and Ram, R.P. (2013), "Effect of activating agents on the activated carbons prepared from lapsi seed stone", *Res. J. Chem. Sci.*, **3**(5), 19-24.

Schaubeder, J.B., Guizani, C., Selinger, J., Mautner, A., Hummel, M. and Spirk, S. (2023), "Design of experiments as a tool to guide the preparation of tailor-made activated carbons", *Sci. Rep.*, **13**(1), 3977. https://doi.org/10.1038/s41598-023-30642-8

Sevilla, M. and Mokaya, R. (2014), "Energy storage applications of activated carbons: supercapacitors and hydrogen storage", *Energy Environ. Sci.*, **7**, 1250-1280. https://doi.org/10.1039/C3EE43525C.

Shao, J., Wang, Y., Liu, C., Xiao, Q., Demir, M., Al Mesfer, M.K., ... and Hu, X. (2025), "Advanced microporous carbon adsorbents for selective CO_2 capture: Insights into heteroatom doping and pore structure optimization", *J. Anal. Appl. Pyrolysis*, **186**, 106946. https://doi.org/10.1016/j.jaap.2024.106946

Shell, S.V., Horsfall, M., Verla, E., Spiff, A. and Ekpete, O. (2012), "Preparation and characterization of AC from fluted pumpkin (Telfairia Occidentalis Hook. F) seed shell", *Asian J. Natural Appl. Sci.*, **1**, 39-50.

Shrestha, R.M. (2017), "Characterization of activated carbons prepared from a locally available material by iodine number". *J. Inst. Eng.*, **13**(1), 139-144. https://doi.org/10.3126/JIE.V13I1.20359

Soelberg, N. (2007), "Off-Gas Mercury Control Using Sulfur-Impregnated Activated Carbon – Test Results", 1-15. https://www.osti.gov/biblio/912449

Sugumaran, P., Susan, V., Ravichandran, P. and Seshadri, S. (2012), "Production and characterization of AC from banana empty fruit bunch and delonix regia fruit pod", *J. Sust. Energy Environ.*, **3**, 125-132.

Vernon-Parry, K.D. (2000), "Scanning electron microscopy: An introduction", *III-Vs Review*, **13**(4), 40-44. https://doi.org/10.1016/S0961-1290(00)80006-X

Won, M., Cho, W., Chang, J.M., Soo, P.J. and Lee, J.Y. (2022), "Characterization of waste wood biochar-based activated carbon synthesized by hydrothermal carbonization", *J. Korea Soc. Waste Manage*, **39**(3), 280-289. https://doi.org/10.9786/kswm.2022.39.3.280

Wong, S., Ngadi, N., Inuwa, I. and Hassan, O. (2018), "Recent advances in applications of AC from biowaste for wastewater treatment: A short review", *J. Clean. Prod.*, **175**, 361-375. https://doi.org/10.1016/J.JCLEPRO.2017.12.059.

Xu, Q., Wang, J., Feng, J., Liu, C., Xiao, Q., Demir, M., ... and Hu, X. (2025), "D-glucose-derived S-doped porous carbon: Sustainable and effective CO2 adsorption", *Colloids Surf. A*, **709**, 136054. https://doi.org/10.1016/j.colsurfa.2024.136054

Yahya, M., Al-Qodah, Z. and Ngah, C. (2015), "A review of agricultural bio-waste materials as potential sustainable precursors for AC production", *Renew. Sust. Energy Rev.*, **46**, 218-235. https://doi.org/10.1016/J.RSER.2015.02.051.

Yunus, N. (2020), "Activated carbon: A versatile material for environmental applications", *J. Environ. Chem. Eng.*, **8**(5), 103997.

Yunus, Z.M., Yashni, G., Al-Gheethi, A., Othman, N., Hamdan, R. and Ruslan, N.N. (2022), "Advanced methods for AC from agriculture wastes, a comprehensive review", *Int. J. Environ. Anal. Chem.*, **102**(1), 134-158. https://doi.org/10.1080/03067319.2020.1717477

Zhang, X. and Huang, Y. (2019), "Preparation method of AC for measuring gas mercury and activated carbon",

1235-1242. https://doi.org/10.1016/j.cej.2018.10.134
Zhi, Y., Shao, J., Liu, C., Xiao, Q., Demir, M., Al Mesfer, M.K., ... and Hu, X. (2025), "High-performance CO2 adsorption with P-doped porous carbons from lotus petiole biomass", *Sep. Purif. Technol.*, **361**, 131253. https://doi.org/10.1016/j.seppur.2024.131253

CC

Abbreviations

AC: Activated Carbon
CHNSO: Carbon-Hydrogen-Nitrogen-Sulfur-Oxygen
FTIR: Fourier Transform Infrared Spectroscopy
SEM: Scanning Electron Microscopy
H_3PO_4: Phosphoric Acid